Polymer Testing 106 (2022) 107449

Contents lists available at ScienceDirect

Polymer Testing

journal homepage: www.elsevier.com/locate/polytest

Rotational molding of polylactide (PLA) composites filled with copper slag as a waste filler from metallurgical industry

Mateusz Barczewski [a,*], Aleksander Hejna [b], Joanna Aniśko [a], Jacek Andrzejewski [a], Adam Piasecki [c], Olga Mysiukiewicz [a], Małgorzata Bąk [d], Bartosz Gapiński [e], Zaida Ortega [f]

[a] Poznan University of Technology, Faculty of Mechanical Engineering, Institute of Materials Technology, Piotrowo 3, 61-138, Poznan, Poland
[b] Gdansk University of Technology, Faculty of Chemistry, Department of Polymer Technology, Narutowicza 11/12, 80-233, Gdansk, Poland
[c] Poznan University of Technology, Faculty of Materials Engineering and Technical Physics, Institute of Materials Engineering, Piotrowo 3, 61-138, Poznan, Poland
[d] Bydgoszcz University of Science and Technology, Faculty of Chemical Technology and Engineering, Seminaryjna 3, 85-326, Bydgoszcz, Poland
[e] Poznan University of Technology, Faculty of Mechanical Engineering, Institute of Mechanical Technology, Piotrowo 3, 61-138, Poznan, Poland
[f] Universidad de Las Palmas de Gran Canaria, Departamento de Ingeniería de Procesos, Edificio de Ingenierías, Campus universitario de, Tafira Baja, 35017, Las Palmas, Spain

ARTICLE INFO

Keywords:
PLA
Polylactide
Rotational molding
Copper slag
Waste filler

ABSTRACT

The research work carried out so far indicates the ever wider possibilities and demand for shaping composite products in the rotational molding technology. This trend was the main reason to use waste-based filler from the metallurgical process as a filler for manufacturing polylactide (PLA)-based remolded composites. Copper slag (CS) was introduced in the single-step processing method to PLA matrix at 5, 10, 20, and 35 wt%. The rotomolded composites with different filler content were subjected to in-depth structural analysis discussed in relationship with mechanical and thermomechanical properties changes. Evaluation of the composite structures by scanning electron microscopy (SEM) and 3D computed tomography (3D CT) analyses showed that incorporating up to 10 wt% of the filler did not cause adverse changes in the filler dispersion in the product volume, which was homogeneous. Lack of unfavorable structural changes in composites with concentrations of up to 20 wt% was related to the rheological properties of the composition. Except for series with the highest filler content (35 wt%), the produced composites were characterized by increased stiffness and hardness than rotomolded parts made from pure PLA. Despite the deterioration of the tensile strength of composite materials using higher filler concentrations, the mechanical performance of 5 and 10 wt% showed an acceptable level while increasing the stiffness by about 15% compared to neat PLA. Moreover, it was shown that the interfacial adhesion between PLA and CS, despite the lack of surface modification of the filler waste, was advantageous.

1. Introduction

Rotational molding or rotomolding is currently one of the most dynamically developing technologies used for thermoplastic polymer processing to produce large-size products. The possibility of almost waste-free shaping of thin-walled parts with favorable mechanical properties means that this technology in many cases has allowed to replace thermoset-based laminates reinforced with inorganic fibers, characterized by limited recycling possibilities after the end of the product life cycle with more sustainable options [1,2]. The undoubted advantages of the rotational molding technology include the relatively low costs associated with starting production, the ability to manufacture products with complex shapes, requiring no post-assembly procedures, no residual stresses in final products, and the ability to obtain many products of various shapes in one production cycle [3]. At the same time, one should remember the disadvantages of the process, which include high energy and time consumption, and in the case of using thermoplastic polymers, the necessity to use materials with appropriate thermal and thermo-oxidative stability [2,4]. While polyethylene is still the most persistent polymer in the rotational molding technology, more and more attempts in the shaping of products made of biodegradable polymers such as polylactide (PLA) or poly(ε-caprolactone) (PCL) and their composites have been undertaken in recent years [5–8]. The most outstanding attention was paid to the processing of PLA as a biopolymer

* Corresponding author.
E-mail address: mateusz.barczewski@put.poznan.pl (M. Barczewski).

https://doi.org/10.1016/j.polymertesting.2021.107449
Received 17 October 2021; Received in revised form 15 November 2021; Accepted 10 December 2021
Available online 11 December 2021

with relatively high availability and which allows a comprehensive modification of its structure, as well as showing good thermal stability [9].

The production of polymer composites, regardless of the type of technology used, injection, extrusion, or rotational molding, allows both to increase the range of applicability of the base materials conventionally used and reduce the price of final products [10–12]. Due to the shaping of the material in the form of a powder, the addition of the particle-shaped filler became a perspective and a justified solution. Two-step preparation of the polymer composition, taking into account preliminary melt processing and further pulverization, allows to obtain products characterized with better mechanical performance; however, one-step production with the simultaneous use of waste material allows to reduce the energy consumption of the process and the overall environmental impact of the production [13,14].

Considering so far published works, lignocellulosic fillers are often introduced into thermoplastics processed by rotational molding. The addition of such fillers as plant fibers (agave [15,16], cabuya, sisal [17], and flax [18]) and other woody parts of plants (wood flour [19], ground husks and hulls [20], and another wooden parts of the plants [21,22]), allows to obtain more sustainable products. However, this procedure is often associated with a significant deterioration of the properties of the final products. The most significant benefit of using inorganic fillers compared to lignocellulosic in the case of rotomolding is the possibility of using the process temperature exceeding 200 °C. In the case of lignocellulosic materials, there is a significant risk of degradation outbreaks during long-term exposure to high temperatures in the range of lignin degradation (above 160 °C) [23]. Therefore, from the point of view of the thermally stable implementation of the technological process, the use of inorganic fillers is more justified.

Several studies concerning modification of thermoplastic polymers using inorganic thermally stable or waste-originated fillers showed high potential in this solution [24–27]. Butora and coworkers [27] discuss the possibility of manufacturing rotational molded linear low-density polyethylene composites filled with 10 wt% of talc. Their investigations showed that it is possible to incorporate a higher amount of the inorganic filler; however, its presence caused deterioration of the mechanical properties. In a series of different studies [24,25], fumed silica was discussed as a potential inorganic filler for rotomolding purposes, reducing the pin-hole effect and increasing the elasticity modulus of LLDPE.

In the case of the lower filler content (1–2 wt%), the processing parameters such as temperature and rotational speed have a dominant role in the mechanical properties of final products [28]. The higher content of the filler, the more distinct impact of final properties is related to geometry and the physicochemical properties of the non-polymeric part of the composite [13,29]. In addition to the appropriate thermal stability of the fillers introduced into the polymer matrix, the method of mixing the components, the size of the filler particles, their aspect ratio, and moisture content are crucial factors from the moldability point of view [13,14,30]. An attempt to produce composites with a higher degree of filling while using the most uncomplicated possible procedure of preliminary filler preparation is essential because it allows for the maximum limit of the amount of used polymer. Simultaneously, it should be realized that direct application of the dry-blended polymer and a filler characterized by large particle size distribution during the rotational molding process may cause agglomeration of the filler [13].

Slag is the term used to describe the totality of non-metallic co-products generated in the production of metals from their ore. The chemical composition largely depends on the type of smelted metal and the smelting technology [31]. Copper slag (CS) is a non-ferrous slag made in the process of ores smelting. Considering that 2 tons of slag are generated for each ton of metal, and the production and consumption of non-ferrous metals and their alloys increases each year, the management of post-production waste becomes a burning problem necessary to solve [32]. Due to the commonness of copper processing, the resulting by-product generates waste in large amounts, which, despite various management methods, still constitutes a developmental material from the point of view of a waste valorization [31]. One of the most common applications related to the management of CS waste is production of abrasives [33], which is justified due to its high hardness, i.e., 6 in Mohs scale [32]. The second main way of managing CS waste today is to use it as a fine aggregate for bituminous mixes and as concrete additive [34,35]. The last application results from the pozzolanic activity, which decreases the heat of hydration more efficiently than fumed silica in mortars. It also increases concrete strength after partially replacing the cement in the concrete composition [32]. Due to the necessity to maximize the use of by-products so that they do not end up as landfill waste, there have been several attempts in the literature to produce polymer composites using copper slag as a filler, for thermosetting polymers such as epoxy [36] and polyester resins [37], and thermoplastics, including the biodegradable ones (PCL) [38].

The chemical composition of copper slag is largely similar to that of fossil mineral materials such as basalt or obsidian [32]. It consists of inorganic chemical compounds, including SiO_2, Al_2O_3, CaO, Na_2O, FeO and Fe_2O_3, MgO, and K_2O [38]. None of the listed materials reveals a biocidal activity that could limit enzymatic biodegradation in the later stages of the biodegradation process [39]. However, due to its hydrophilicity, its presence increases the possibility of PLA degradation in the initial degradation period, dominated by hydrolytic degradation [40,41]. While it is preferable to reuse copper slag waste, significant amounts are disposed of by deposition on landfills [31]. Therefore, despite the lack of the possibility of full biodegradation (filler decomposition), it is assumed that after the end of the life cycle of PLA-CS composites, it will be possible to realize the composting process, and the inorganic residue will not constitute a burden for the natural environment. At the same time, compared to PLA-based composites produced using lignocellulosic fillers, it is possible to shape products at a temperature above 200 °C, without the risk of thermal decomposition of the reinforcement.

While the use of waste fillers is one of the more dynamically developed concepts of the possibility of shaping sustainable materials, relatively few studies describe the use of waste materials as fillers for composites formed in the rotational molding process. As it was mentioned earlier, most researchers focus on the development of shaping rotomolded products reinforced with lignocellulosic fillers, including waste from the agricultural and food industries [30,42] or natural fibers with a limited scope of use, such as banana or agave fibers, which were, among others, incorporated into the polyethylene matrix [43,44].

Considering the results of earlier works involving the use of CS as a waste filler for the production of composites with a matrix of various polymers, including the thermoplastic and the thermosetting ones, the attempt to use this waste powder filler in the rotomolding technology seems to be justified. Moreover, the amount of work on the use of non-lignocellulosic waste fillers for the production of rotomolded composites is limited and refers mainly to ground tire rubber [45] or basalt powder [46]. This study aims to assess the possibility of shaping biodegradable polyester filled with copper slag as a raw waste filler from the metallurgical industry by the single-stage method, using dry-blend preprocessing. The conducted research allows to correlate the amount of introduced waste material with the emerging product defects and quality features, assessed through a multi-criteria structural and thermal analysis related to the mechanical and thermomechanical properties of the final composites.

2. Experimental

2.1. Materials

The commercial polylactide grade PLA RXP 7501 from Resinex, Warszawa, Poland, (MFI = 75 g/10 min, 190 °C/2.16 kg) in powder

form was used as a polymeric matrix for manufacturing of rotomolded parts and composites. The use of the low melt viscosity polymer was deliberate and aimed at minimizing the adverse effects of the presence of the inorganic filler introduced by the direct method.

Copper slag (CS), as a by-product generated from a suspension furnace, was derived in the form of fine powder with a grain density of 3.04 g/cm^3 from Polish copper-rich deposits. The chemical composition of CS, as declared by the supplier, consist of: 41.2 wt% SiO_2, 19.1 wt% Al_2O_3, 13.1 wt% CaO, 12.0 wt% Fe_2O_3 + FeO, 4.9 wt% MgO, 1.1 wt% Cu. The material shows a moisture content of 0.13 wt%. Particle size distribution of CS and SEM images of the filler are presented in Fig. 1. Broader information about the used filler was presented in a previous work [38].

2.2. Sample preparation

Before processing, the PLA powder with particle-shaped waste inorganic filler portions was preliminary mixed for 5 min using a high-speed knife mill Retsch GM 200 with the rotational speed of 2000 rpm. After that, portions of PLA with 5, 10, 20, and 35 wt% of CS were subjected to drying under a Chemland vacuum cabinet drier at 70 °C for 24 h. The total amount of material used for the manufacturing of each part was 150 g. The rotational molding process was carried out using the single-spindle shuttle rotational molding machine REMO GRAF (Poland) with two rotation axes, equipped with 185 × 60 × 60 mm cuboid-shaped steel mold. A detailed description of the used machine was presented in our previous work [19]. After introducing a measured amount of polymer and filler, the sealed mold was introduced into the heating chamber of the machine. The rotomolding process was done with the ratio of the rotational speed of axes of 1:3, and the set of processing parameters that allows obtaining the constant measured temperature in the oven during the processing of 250 °C, rotation time at elevated temperature was 20 min, and 20 min cooling time using the forced airfield. All samples assigned as PLA in this study are materials taken from products processed in the rotational molding technology, manufactured in the same conditions and preprocessing procedure as PLA-CS composite series.

2.3. Methods

The Fourier Transform Infrared spectroscopy (FT-IR) was conducted using a spectrometer Jasco FT/IR-4600, operating at room temperature (23 °C) in a mode of Attenuated Total Reflectance (ATR - FT-IR). A total of 64 scans at a resolution of 4 cm^{-1} was used in all cases to record the spectra.

Thermogravimetric analysis (TGA) was employed to study the thermal degradation of the PLA and the composites. The samples of 10 ± 0.2 mg placed in Al_2O_3 crucibles were heated in the temperature range of 30–900 °C with a rate of 10 °C/min, using a Netzsch TG209 F1 apparatus. An inert atmosphere of nitrogen was applied. Based on the obtained mass vs. temperature curves, its first derivative (dTG) was calculated. Values of 5, 10, and 50% mass loss ($T_{5\%}$, $T_{10\%}$, and $T_{50\%}$) and residual mass were determined.

The thermal properties of the studied materials, such as melting, crystallization, and cold crystallization temperature (T_m, T_{cr}, and T_{cc}, respectively) and the crystallinity degree, were analyzed using the differential scanning calorimetry (DSC) method. Samples of 5 ± 0.2 mg were placed in aluminum crucibles with pierced lid and heated from −30 °C to 200 °C with a rate of 10 °C/min, held at this temperature for 10 min and then cooled back to −30 °C with a rate of 10 °C/min. This heating/cooling cycle was performed twice. As the samples prepared in the same way had a similar thermal history, the first heating/cooling and second heating cycles information were used in the analysis. A Netzsch DSC 204F1 Phoenix apparatus and a nitrogen atmosphere were used. The crystallinity degree (X_{CR}) was calculated according to equation (1):

$$X_{CR} = \frac{\Delta H_M - \Delta H_{CC}}{(1-\varphi)\cdot\Delta H_{PLA100\%}}\cdot 100\% \quad (1)$$

where: ΔH_M – melting enthalpy of the sample, ΔH_{CC} – cold crystallization enthalpy of the sample, $\Delta H_{PLA100\%}$ - melting enthalpy of a 100% crystalline PLA, $\Delta H_{PLA100\%} = 93.7$ J/g [47], φ – filler content.

Rheological investigations were carried using an Anton Paar MCR 301 rotational rheometer, with 25 mm diameter parallel plates and a 1.5 mm gap under the oscillatory mode. The experiments were conducted at 200 °C. Before performing the dynamic oscillatory measurements in the frequency sweep mode, the strain sweep experiments were conducted. The strain sweep experiments of all the samples were performed at 200 °C with a constant angular frequency of 10 rad/s in the varying strain window 0.01–100%. The preliminary investigations allow to determine the value of 0.5% strain as applicable for frequency sweep experiments and located for all samples in the linear viscoelastic (LVE) region. The angular frequency used during the studies was in the range of 0.05–500 rad/s.

The specific weight of applied fillers and resulting composites was determined using Ultrapyc 5000 Foam gas pycnometer from Anton Paar (Graz, Austria). The following measurement settings were applied: gas – nitrogen; target pressure −18.0 psi; flow direction – sample first; temperature control – on; target temperature – 20.0 °C; flow mode – monolith; cell size – medium, 45 cm^3; preparation mode – flow, 0.5 min; the number of runs – 10.

The results obtained from pycnometry measurements were used to determine the porosity of composites as the difference between theoretical and experimental values of density. Theoretical values were calculated according to equation (2):

$$\rho_{theo} = \rho_m \cdot (1-\varphi) + \rho_f \cdot \varphi \quad (2)$$

where: ρ_{theo} – theoretical density of the composite, g/cm^3; ρ_m – density of the matrix – 1.2515 g/cm^3; ρ_f – density of the filler – 3.0400 g/cm^3; and φ – a volume fraction of the filler.

To quantitatively determine the composite's porosity, equation (3) was applied as follows:

$$p = \frac{\rho_{theo} - \rho_{exp}}{\rho_{theo}}\cdot 100\% \quad (3)$$

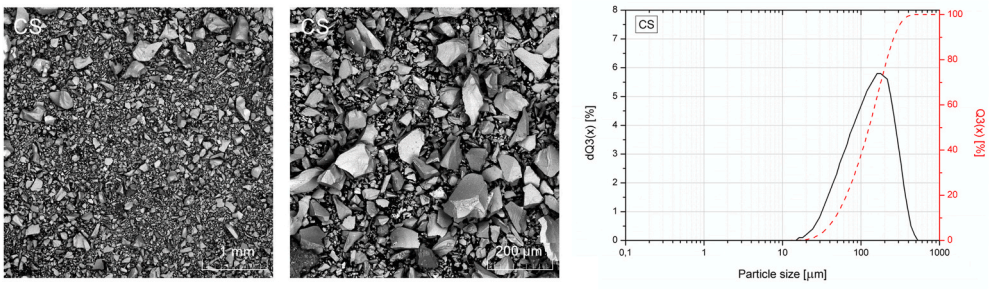

Fig. 1. Particle size distribution and SEM image of copper slag.

where: p – porosity of the material, %; and ρ_{exp} – an experimental value of density of composite, g/cm^3.

The structure of the composite samples was examined with the use of a measuring X-ray tomography, model v|tome|x s240 (Waygate Technologies/GE Sensing & Inspection Technologies GmbH). The use of micro-computed tomography (μCT) was focused on evaluating the distribution of the filler agglomerates and wall thickness. Following scanning, parameters were used during the measurements - micro focus x-ray tube (voltage 150 kV/current 200 μA); the exposure time for one picture was 150 ms, and the voxel size was 123 μm.

The scanning electron microscope (SEM) Tescan MIRA3 (Brno, Czech Republic) was used to assess the structure of the PLA and PLA-based composites formed by rotational molding. The brittle fractured samples were assessed with an accelerating voltage of 12 kV and a working distance of 16 mm. A thin carbon coating with a thickness of approximately 20 nm was deposited on samples using the Jeol JEE 4B vacuum evaporator. The microscope was equipped with an EDS-UltimMax energy-dispersive spectrometer (Oxford Instruments, High Wycombe, UK) and Aztec Energy Live Standard software, which allow the determination of the oxygen content at the evaluated surface.

The tensile properties of PLA and its composites were determined using a Zwick/Roell 010 universal testing machine, according to ISO 527 standard. The crosshead speed was set to 1 mm/min during the tensile modulus evaluation and 10 mm/min in the remaining part of the test. Based on the obtained data, values of tensile modulus (E), tensile strength (R_m), and elongation at break (ε) were determined. At least five samples of each kind were tested.

The ball indentation hardness of the composite samples and pure PLA was measured using a KB Prüftechnik tester, according to ISO 2039 standard.

The impact strength was evaluated using the Dynstat method in compliance with the DIN 53435 standard on unnotched samples with dimensions of 4 × 10 × 15mm. A Dys-e 8421 apparatus equipped with a 0.98 J hammer was employed.

Thermomechanical properties of the copper slag powder-filled samples and PLA were evaluated by Dynamic Mechanical Thermal Analysis (DMTA) using an Anton Paar MCR 301 apparatus operating in the torsion mode. The samples were heated from 25 °C to 120 °C with a rate of 2 °C/min. The strain of 0.01% was applied at a frequency of 1 Hz.

The Vicat softening temperature (VST) was evaluated according to the standard ISO 306, using a Testlab RV300C with a heating rate of 2 °C/min, and a load of 10 N was applied.

3. Results and discussion

Fig. 2 shows the FTIR spectra of CS, PLA, and PLA-CS composites. In the case of the filler, the most significant were the absorption bands in the fingerprint region derived from Si–O stretching (940 cm^{-1}) and Si–O/Al–O bending vibrations (460 cm^{-1}) [48,49]. PLA and its composites spectra contained absorption bands characteristic for this biodegradable polyester, i.e., OH stretching (3504 cm^{-1}), asymmetric and symmetric CH stretching (2997 and 2946 cm^{-1}), –CH_2 asymmetric and symmetric stretching from aliphatic group (2920 and 2851 cm^{-1}), CH stretching (2877 cm^{-1}), C═O stretching (1748 cm^{-1}), CH_3 asymmetric bending (1452 cm^{-1}), CH deformation (1382 cm^{-1}), CH asymmetric band (1360 cm^{-1}), CH bending (1315 and 1300 cm^{-1}), CO stretching (1264 cm^{-1}), CO- stretching in –CH–O– (1178 cm^{-1}), –COC stretching (1130 cm^{-1}), OC asymmetric stretching mode (1090 cm^{-1}), C–OH side group vibration (1041 cm^{-1}), helical backbone with CH_3 rocking modes (956 and 921 cm^{-1}), and bands related to PLA crystalline and amorphous phases (940 and 460 cm^{-1}) [50–54]. FTIR -ATR measurements were made for the external surface of the part. The absence of bands characteristic for CS in the case of all composites proves the correct course of the technological process. The outer wall of the product was firstly covered with a thermoplastic polymer layer, which was confirmed by the lack of additional overlapping peaks from the filler on the spectra of the composite samples. Also, in polymer samples, no peak growth was observed at 1748 cm$^{-1,}$ corresponding to carbonyl groups. In the case of intense thermo-oxidation processes, an increase in intensity within this band [55] or the appearance of an additional inflection of about 1713 cm^{-1} originating from the stretching of COOH [56] are usually observed. In the case of composite samples, only a decrease in the value in the discussed range was recorded. Therefore it can be concluded that FTIR spectra show no degradative effects, or as it will be discussed in the following parts of the manuscript, this method was insufficiently sensitive to measure the degradative changes taking place as an effect of processing.

Based on the TGA results presented in Fig. 3 and Table 1, it can be observed that the degradation of PLA and PLA-CS composites is a one-step process, and the addition of the filler only causes a reduction in composites thermal stability in comparison to pure PLA, shifting the degradation onset temperature to lower values: the greater the content of inorganic filler in the composite, the lower is the onset temperature. However, it should be emphasized that the nature of the degradation process represented by the curve has not changed. Considering the negligible influence of shear forces and the implementation of the process in the temperature range of the confirmed thermal stability of PLA and filler, the observed decrease in thermal stability in TG thermograms and the values at selected mass losses are originated from the presence of the filler. A similar effect of thermal stability reduction was noted for PCL composites filled with CS [38] as well as for PLA-based composites filled with different inorganic fillers [57–59]. It should be underlined that degradation occurs in a lower but similar temperature range. Considering the physicochemical properties and the chemical structure of the copper slag, it can be assumed that the observed reduction in

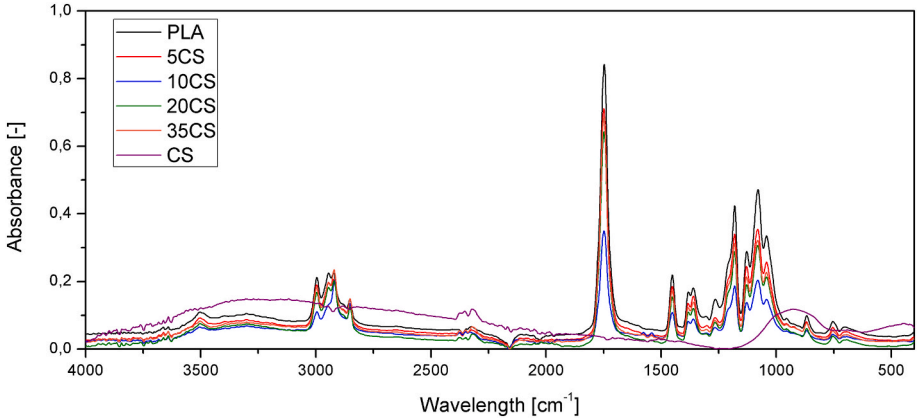

Fig. 2. FTIR spectra of PLA, PLA-CS composites, and filler.

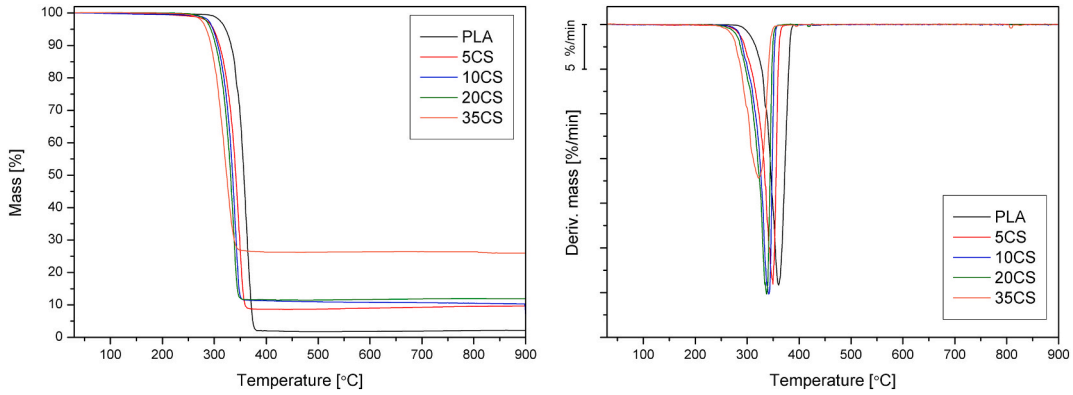

Fig. 3. TG and DTG curves of PLA and PLA-CS.

Table 1
Thermal properties of PLA and PLA-CS composites obtained from TGA.

Material	$T_{5\%}$	$T_{10\%}$	$T_{50\%}$	DTG peak	Residual mass
	[°C]			[%/min; °C]	[%]
PLA	321.9	332.5	356.9	29.14; 360.4	2.17
5CS	298.7	310.3	341.4	29.04; 349.7	9.69
10CS	297.6	307.0	335.2	30.18; 341.3	10.28
20CS	293.3	302.7	331.2	30.18; 337.5	11.88
35CS	284.6	293.7	323.8	17.17; 321.7	25.98
CS	–	–	–	–	98.51

thermal stability is related to two simultaneous mechanisms. On the one hand, hydrolytic degradation of PLA may occur during processing due to the release of not completely removed residual water from the highly hygroscopic filler [13]. The second mechanism of polymeric matrix degradation, resulting in lower thermal stability, can be attributed to presence of metal oxides in the waste-based filler structure. The literature describes [57,60–62] the effects of alkaline metal oxides and metallic ions that could catalyze the depolymerization or intermolecular transesterification reactions of the PLA in a temperature range similar to that used during processing (up to 230 °C). If the values of the DTG curve maximum are analyzed, it can be seen that only for 35CS the intensity of maximum degradation rate was lowered, which should be related to the lower amount of the polymer. For all materials, the onset degradation ($T_{5\%}$) values significantly exceed the molding and use temperature of the composites. Therefore, it can be concluded that the observed adverse changes will not deteriorate the application properties of the final rotomolded parts made of PLA-CS composites.

Additionally, differential scanning calorimetry (DSC) analyses were conducted. However, the used PLA matrix showed almost completely amorphous behavior, and no significant changes of thermal properties, including characteristic temperatures of melting and glass transition, were observed. The nucleating ability of CS on used PLA grade was negligible, and the observed changes in mechanical and thermo-mechanical properties cannot be related to changes in the crystalline structure of the polymeric matrix. The DSC results were presented collectively in supporting information (Fig. 1S and Table 1S).

The assessment of rheological properties in the oscillation mode was aimed to provide information allowing to understand structural changes in rotationally molded parts. Fig. 4 shows the changes in storage and loss modulus as a function of angular frequency and complex viscosity curves made for PLA and PLA-CS composites. Due to the selection of PLA grade with low viscosity, the addition of the filler even in the highest amount did not change the dominant viscous behavior in the entire considered angular frequency range, which reflects the real shearing conditions during the rotational molding [63]. All composites showed a different course in low angular frequencies range than the unmodified PLA sample due to the partial hindering of the polymeric macromolecules by the filler particles [64,65]. However, it should be noticed that no plateau formation was observed for any samples that could indicate the formation of a 3D agglomerated filler structure throughout the sample volume. In the analyzed range, the changes, despite the partial deflection of the G′(ω) curves, did not become fixed and independent of the ω in a small angular frequency range.

It is assumed that there is a correlation between zero viscosity (in the low shear rate range) and the ability to air bubbles removal [66]. It is difficult to eliminate air residues resulting from the process of polymer powder sintering from a material characterized by very high viscosity and melt strength. All curves showed a Newtonian plateau in the range of low angular frequencies, only for 35CS slight inflection and increase of η* below 0.5 rad/s was denoted, which is related to immobilization of agglomerated clusters of the filler in polymer melt [67]. For composites containing 5 and 10 wt% of CS, a decrease in the viscosity of the

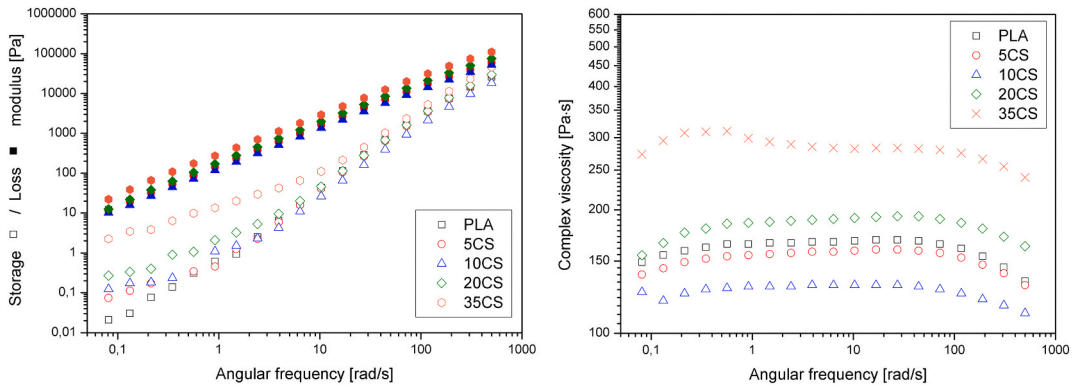

Fig. 4. Oscillatory rheology results; storage/loss modulus and complex viscosity vs. angular frequency of PLA and PLA-CS composites.

formulations was noted in the entire considered range, while a further increase in the filler content resulted in a reversal of this trend. However, it should be emphasized that considering the range of viscosity changes, only for the 35CS sample, the increased viscosity values can be considered significant and impact the actual formation of structural defects in the product (as seen in Figs. 5–7). In the analyzed case, the measurements were performed by lowering the angular frequency. Therefore, the reduction of the complex viscosity in the range of small angular frequencies may result from partial thermo-oxidation of the polymer. Considering the reduced thermal stability of the composites caused by the introduction of the filler, which was attributed to hydrolytic degradation and possibly depolymerization effects, the changes in the viscosity of composites containing 5 and 10 wt% of filler seem to be understandable. When over 20 wt% of CS was introduced into PLA, the viscosity reduction due to the polymer degradation was dominated by the effect of rigid filler structures presence. As a result, the increase of the complex viscosity compared to unmodified rotationally molded PLA for 20CS and 35CS series was noted.

The visual appearance of rotational molded parts made of PLA and PLA with different CS content is presented collectively in Fig. 5. It can be observed that in the case of a composition containing 10 wt% or more of CS, the products obtain a uniform color, while defects in the form of pin-holes are only observed for the 20CS composition. Only for the part produced using the highest concentration composite, the loss of continuity of the structure in the central part of the product walls was denoted.

Fig. 6 shows a summary of the results of the 3D CT analysis, which consists of the tested sample 3D model, its structure including wall thickness, and the distribution of the filler particles, respectively. Considering the high ability of CS to create agglomerates during melt processing, resulting in the creation of product cohesion deficiencies in the form of macroscopic holes observed in 20CS and 35CS composites, the limited moldability of PLA-CS composites at high filler content may be defined. In the case of a composite containing 5 wt% of CS, the wall thickness was more uniform compared to the unmodified PLA. Further increasing the proportion of the filler caused the formation of thinning in the central point of the sidewalls of the parts. The second of the performed analyzes included the determination of the filler dispersion in the PLA matrix. One can observe a variable tendency in the distribution of the CS particles in the volume of the part. For 5CS and 10 CS composites, the filler is located mainly in the walls and is characterized by relatively good dispersion. The higher filler content was characterized by an increased proportion of agglomerated domains in the corners of the product. Simultaneously, this effect with the unacceptable intensity was noted only for the sample with the highest filler amount.

Fig. 7 presents the impact of filler loading on the density and porosity of prepared materials. Clearly, the incorporation of the inorganic filler with relatively high specific gravity caused a significant increase in PLA density. Nevertheless, differences between the theoretical density, calculated using the rule of mixture, and the experimental values were noted. Such an effect was attributed to composites' structure's porosity and is often noted for polymer-based composite materials [68]. Generation of voids inside the composites' structure can be attributed to the imperfect interface between matrix and filler particles, as well as to the air inclusions due to the filler agglomeration [69]. The first issue is mostly related to the differences in matrix and filler polarity and insufficient wetting of filler with matrix and can be noted irrespectively of the filler loading. On the other hand, air inclusions rather point to the overloading of the matrix with filler particles or inefficient mixing of phases. Therefore, typically the porosity of composites is increasing with filler content [70,71]. In the presented work, a similar effect was noted up to 20 wt% CS loading. The porosity of 20CS sample almost reached 6%, indicating the increased amount of voids inside the material, which confirmed the results of 3D CT analysis (Fig. 6). Nevertheless, for sample 35CS the porosity was maintained at a similar level. Such an effect could be attributed to the presence of a noticeable amount of pin-holes in the structure of composites, which affects the measurements using gas pycnometry. Due to pin-holes' presence, gas can penetrate the interior of the sample, thus reducing the calculated porosity.

Fig. 8 shows a compilation of the SEM images of the cross-section of rotationally molded parts in the middle of the sidewall. Images were taken in SE and BSE modes (left and right image respectively) to evaluate both the form of fracture and the distribution of CS particles. The external surface of the product is shown on the left image. It should be noticed that not for all the composite samples, the deterioration of the internal surface quality was noted. A visible variation in the sample thickness on the cross-section and deterioration of the quality of the inner surface of thin-walled products, especially for the series with a higher degree of filling, was observed. A similar effect was noted in different studies concerning the addition of talc to rotationally molded LLDPE-based composites [27]. Moreover, although the accumulation of filler particles on the outer surface of the samples was visible for the 20CS and 35CS composites, it did not affect the improper representation of the mold surface. Therefore, it can be concluded that PLA formed a thin layer on the surface of the article in the initial stage of the process. This is in line with the FTIR-ATR results, in the case of which there were no additional absorption bands from the CS, which proves the correct implementation of the process in the initial stage corresponding to the formation of the polymer skin forming the outer layer of the product.

Usually, the introduction of a powder filler results in an increased amount of voids and pores in rotationally molded part due to hindered diffusion of air bubbles resulting from insufficient densification of the composite structure [72] or release of residual moisture and/or volatile degradation components from the filler subjected to long-term heating in the technological process [30]. In the case of PLA composites reinforced with CS, the incorporation of up to 5 wt% of the filler did not provide a significant increase of the porosity, while the calculated porosity values for higher filler content are comparable to data reported for rotomolded products reinforced with inorganic fillers [72], and are at an acceptable level. The relatively bigger inorganic filler particles did

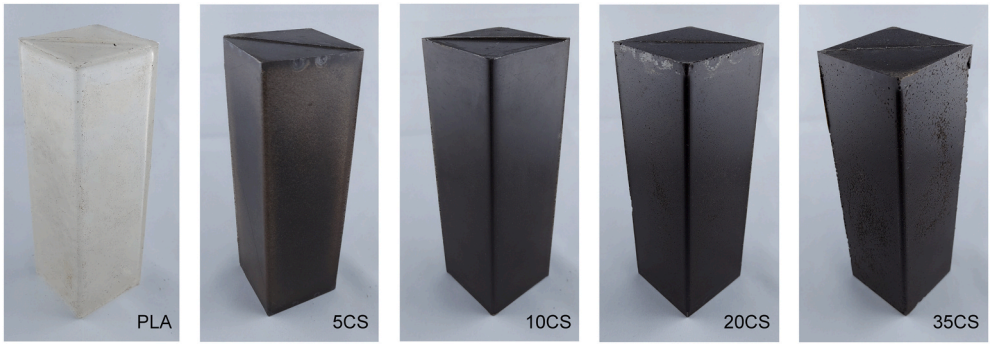

Fig. 5. Visual appearance of rotomolded PLA and PLA-CS composites parts.

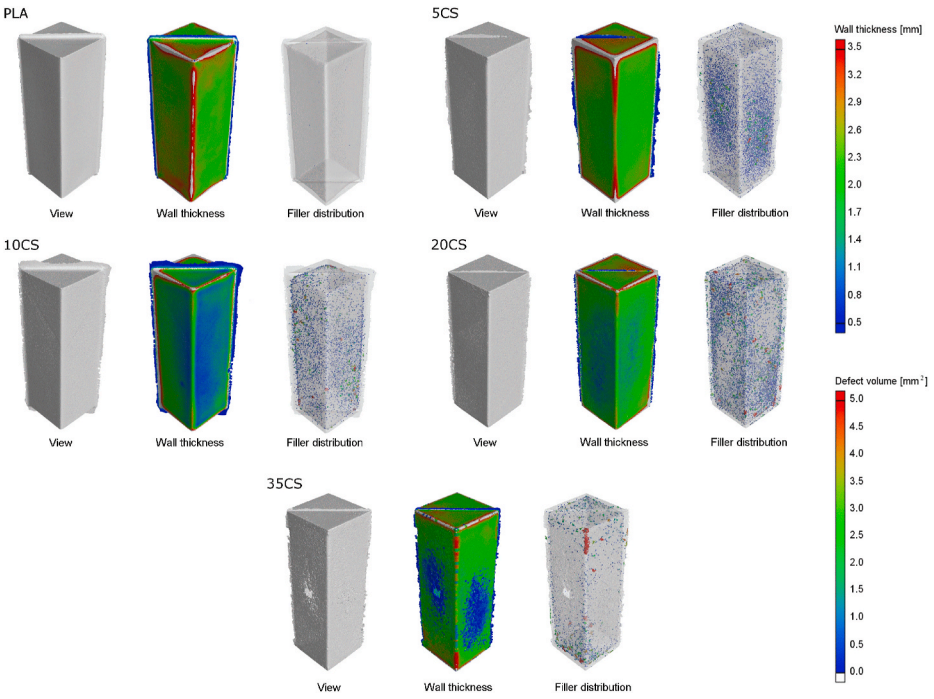

Fig. 6. Results of 3D CT analysis presenting a view of the sample, wall thickness, and filler particles distribution in rotationally molded samples.

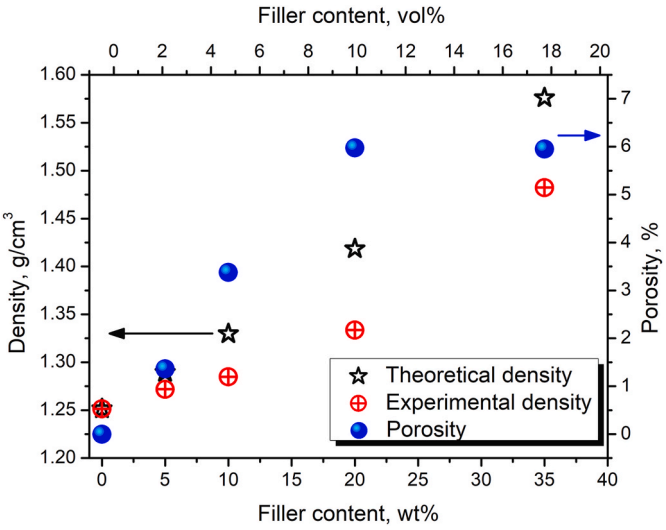

Fig. 7. Values of theoretical and experimental density and porosity of prepared composites.

not adversely affect the entrapment of air domains in the polymer during processing. This phenomenon may also result from the relationship between melt strength and polymer viscosity and the ability to remove air from polymer bulk during rotomolding [28,29] and intensified oxidation of PLA structure through oxygen diffusion direct through the polymer during the densification process [2]. In our case, using low viscosity PLA grade and high processing temperature allows reducing the viscosity of the composite, which allows the air bubbles to diffuse from the polymer melt. Moreover, copper slag is characterized by high thermal resistance and low hydrophilicity. Therefore, the lack of a significant increase in the pore content, which additionally translates into an increase in the wall thickness of the castings, is justified. The analysis of SEM images confirms the results obtained with 3D CT.

SEM images compiled for a composite containing 10 wt% of CS are shown in Fig. 9. The images taken represent the same shot made in the SE, BSE, and EDS techniques. The composite fracture is brittle, which is typical for amorphous or semi-crystalline polymers with a low degree of crystallinity, as confirmed by the results of the DSC analysis. The saturation of the surface of the filler particles by PLA is satisfactory, as no interfacial gap was observed (Fig. 9b). There was no indication of characteristic breakouts due to the pull-out of the CS particles. Thus, it can be concluded that, despite the lack of surface modification, the adhesion at the polymer-filler interface is correct. The use of EDS analysis allows to precisely determine the filler particles' location and confirm its chemical composition given by the producer and described in our previous work [38].

Table 2 shows the results of the mechanical characterization. The filler addition in the amount of up to 20 wt% causes the stiffness increase in comparison to unmodified PLA. The highest value of 2.91 GPa was recorded for the sample containing 10 wt% of the CS. However, the sample containing 35 wt% filler had the lowest Young's modulus among the tested material series, which may be due to the loss of load-bearing capacity of the composite containing significant amounts of agglomerated inorganic filler structures. Polylactide composites produced by introducing an inorganic filler and PLA powder directly into the mold showed reduced mechanical properties compared to the unmodified material. While for composites containing up to 10 wt% there was a relatively small decrease in tensile strength, further increasing the filler content resulted in its drastic drop, reaching 50% of the value compared to the reference sample at 20 wt% of the CS and less than 10% for the composite by the highest degree of filling. While the properties of 20CS can be considered acceptable for less mechanically loaded applications, the use of 35 wt% of CS drastically deteriorates the properties of the composite. Such an effect could be attributed to the reduced homogeneity of material resulting from the presence of voids. A similar tendency was noted for the PCL-CS composites [38], while the samples injection molded and blended in the molten state with a highly flexible polymer matrix showed a lower tendency to weaken the structure by the inorganic powder filler. Even though all samples, due to the amorphous structure, were characterized by low values of strain at break, a clear tendency of this property decreasing with the addition of filler is visible.

The impact strength of composites did not change significantly in comparison to the reference sample. A low impact strength

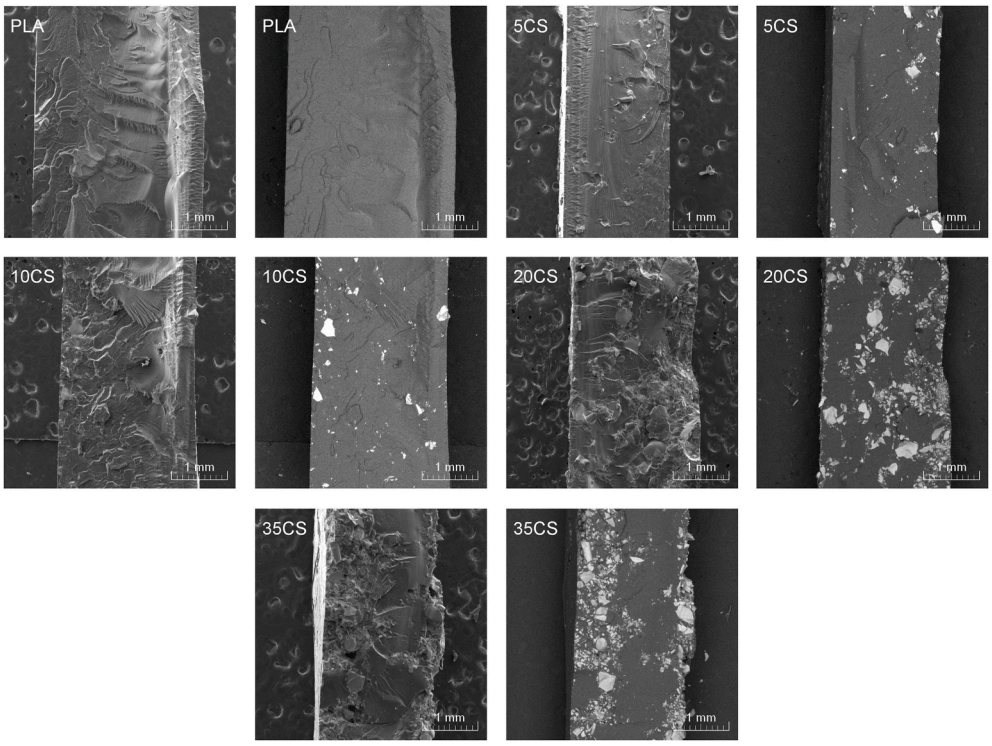

Fig. 8. SEM images of PLA and PLA-CS rotationally molded samples cross-section (external surface from the left side).

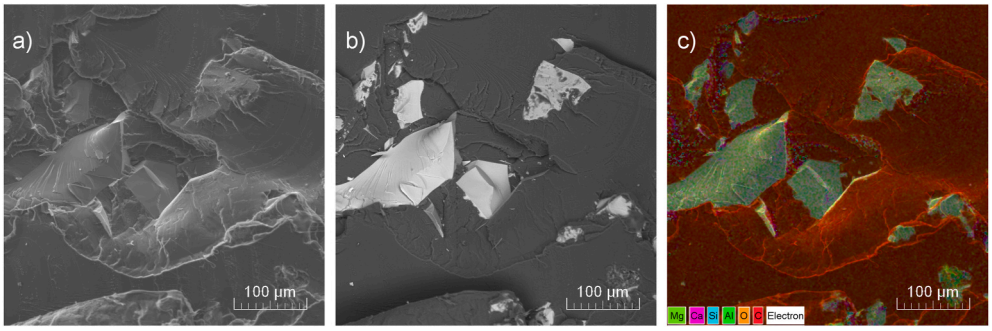

Fig. 9. SEM images of 10CS made using SE (a), BSE (b), and EDS (c) mode.

Table 2
Mechanical and thermomechanical properties of PLA and PLA/CS composites.

Properties	Unit	PLA	5CS	10CS	20CS	35CS
Elasticity modulus	[GPa]	2.39 ± 0.09	2.57 ± 0.1	2.9 ± 0.14	2.81 ± 0.32	1.9 ± 0.57
Tensile strength	[MPa]	53.5 ± 4.4	48.2 ± 0.94	42.6 ± 3.6	27.7 ± 1.6	5.9 ± 2.9
Elongation at break	[%]	2.9 ± 0.36	2.6 ± 0.2	2.00 ± 0.17	1.4 ± 0.08	0.45 ± 0.13
Dynstat impact strength	[kJ/m^2]	5.91 ± 0.67	4.74 ± 0.84	5.96 ± 2.89	4.1 ± 0.89	2.11 ± 1.26
Hardness	[ShD]	69.53 ± 1.18	70.47 ± 3.16	68.87 ± 4.37	73.40 ± 1.96	75.73 ± 2.19

characterized all materials; however, only the 35CS sample shows over 50% decrease in this characteristic compared to unmodified PLA.

The exception in the lowered mechanical performance of composites induced by CS addition was hardness, where even the highest amount of filler caused an increase in this mechanical parameter. Considering that CS consists of 41.2 wt% of SiO_2 and 19.1 wt% of Al_2O_3 [38], which are characterized with Mohs hardness of 7 and 9 respectively [73,74], the changes of final composites hardness induced by increasing content of the inorganic filler are reasonable.

Fig. 10 shows the dynamic thermomechanical analysis results in the conditions of non-destructive dynamic deformations as changes in the storage module (G′) and damping factor (tanδ) as a function of temperature. Additionally, selected DMA data, as well as results of VST tests, are collectively presented in Table 3. The DMA results are in agreement with the results of the tensile mechanical properties and DSC analysis. The highest G′ values were recorded for the 10CS sample, which was also characterized by the highest Young's modulus. In the case of higher filler concentrations, agglomerated filler structures reduced the reinforcing effect, and as a result, no further increase in stiffness in the range below the alpha relaxation was observed. The increase in filler content in the glassy-to-rubbery transition area limited the drop in G′ above the glass transition temperature. The minimum values recorded for 20CS and 35CS were an order of magnitude higher than for the unmodified PLA, which confirms the reinforcing ability of CS particles on the thermoplastic biopolyester matrix. All samples show an intense drop in G′, suggesting no nucleating ability of CS on PLA grade with low ability to create crystalline domains, which is in line with DSC results. The change

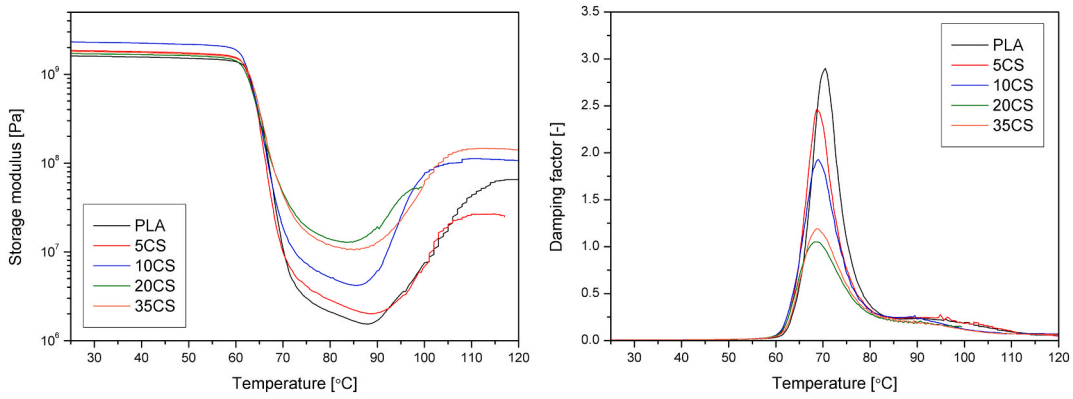

Fig. 10. Results of dynamic thermomechanical analysis; storage modulus and damping factor vs. temperature.

Table 3
Thermomechanical parameters of PLA and PLA-CS composites obtained by DMA and VST.

Material	$G'_{25\ °C}$	$G'_{80\ °C}$	Tg	tanδ at Tg	VST
	[Pa]		[°C]	[−]	[°C]
PLA	$1.61{\cdot}10^9$	$2.12{\cdot}10^6$	70.5	2.90	66.76 ± 0.48
5CS	$1.85{\cdot}10^9$	$2.86{\cdot}10^6$	68.6	2.46	65.68 ± 0.23
10CS	$2.31{\cdot}10^9$	$5.14{\cdot}10^6$	69.0	1.93	67.42 ± 1.51
20CS	$1.71{\cdot}10^9$	$1.39{\cdot}10^7$	68.6	1.05	66.52 ± 0.27
35CS	$1.80{\cdot}10^9$	$1.19{\cdot}10^7$	68.8	1.19	66.07 ± 2.58

in G 'growth in the temperature range above 90 °C, observed for composites with higher filler concentrations, may indicate an increase in the mobility of PLA macromolecules caused by thermo-oxidative phenomena intensified by the presence of CS, and discussed in the thermal stability analysis. Considering the DSC data compiled in the supplementary data (Fig. S1 and Table S1), the increase in the G′ value may be related to the phenomenon of cold crystallization of PLA and its composites [75].

The change in glass transition temperature, read as the maximum of the tanδ(T) curve, caused by the filler additions is negligible. This is understandable given the lack of filler reactivity to PLA and the lack of crystalline structure change in composites. At the same time, a gradual decrease in the maximum value of the damping factor is observed with the increasing share of the filler, reaching the minimum value for 20CS. The reduction in the damping ability is due to the presence of rigid filler particles dispersed in the polymer matrix. The increased tan δ value observed for 35CS is a result of the presence of agglomerated filler structures as well as porosity.

The evaluation of the Vicat softening of the temperature is carried out by static pressing the needle into the tested material, and its result is influenced not only by the structural properties of the polymer, such as the degree of crystallinity and cross-link density but also by the reinforcing effect obtained by the presence of rigid filler structures dispersed in a polymeric matrix. Taking into account the results of previous work, there is a correlation between hardness and VST. Typically, a simultaneous increase in both parameters is observed, including due to the presence of an inorganic powder filler [76,77]. In the considered case, the presence of the filler did not influence Vicat softening temperature. The changes in the recorded values for the individual materials tested are negligible. It is well known that changes in the thermomechanical parameters of PLA are significantly correlated with its crystal structure; for the composite materials produced with an increasing amount of CS, no changes in the degree of crystallinity were noticed, and the presence of the filler did not cause a sufficient reinforcement effect to allow increasing the thermomechanical stability measured in static load conditions. Despite the similar load type, the hardness and VST evaluation show no consistent results, which may be related to a mutually exclusive reinforcing ability of dispersive filler and weakening effect of porosity, observed for composites with higher CS content.

4. Conclusions

In this study, the single-step rotational molding technology was successfully applied to manufacture polylactide-based composites filled with various amounts of copper slag. It was found that the unmodified inorganic waste filler provided good adhesion to the biopolyester matrix and created a uniform composite structure, especially in the case of the lower filler loadings. Moreover, the presence of copper slag did not significantly influence the melting behavior and crystalline structure of the studied material, nor did it provide any major processing difficulties. The application of the inorganic filler did not deteriorate the thermal stability of the studied material, which is its major advantage over lignocellulosic waste fillers. The specimens containing up to 10 wt% of CS were characterized with increased stiffness and hardness. The addition of a higher filler content was also possible. Even though the samples filled presented lower mechanical properties, the composites containing up to 35 wt% of copper slag can still be used for less demanding applications. It can be decided that the production of rotationally molded polymeric composites is a good way to revalorize waste from copper smelting.

Author contributions

Conceptualization: Mateusz Barczewski, Aleksander Hejna, Methodology: Mateusz Barczewski, Aleksander Hejna, Adam Piasecki, Joanna Aniśko, Olga Mysiukiewicz. Formal analysis: Mateusz Barczewski, Aleksander Hejna, Joanna Aniśko, Adam Piasecki, Olga Mysiukiewicz, Zaida Ortega. Investigation: Mateusz Barczewski, Aleksander Hejna, Joanna Aniśko, Adam Piasecki, Olga Mysiukiewicz, Małgorzata Bąk, Bartosz Gapiński, Jacek Andrzejewski, Resources: Mateusz Barczewski, Aleksander Hejna, Writing - Original Draft: Mateusz Barczewski, Aleksander Hejna, Olga Mysiukiewicz, Zaida Ortega, Writing - Review & Editing: Mateusz Barczewski, Olga Mysiukiewicz, Zaida Ortega, Visualization: Mateusz Barczewski, Adam Piasecki, Aleksander Hejna, Olga Mysiukiewicz, Supervision: Mateusz Barczewski, Project administration: Mateusz Barczewski, Aleksander Hejna, Funding acquisition: Mateusz Barczewski.

Declaration of competing interest

The authors declare that they have no known competing financial interests or personal relationships that could have appeared to influence the work reported in this paper.

Acknowledgments and funding

The results presented in this paper were partially funded with grants for education allocated by the Ministry of Science and Higher Education in Poland executed under the subject of No 0613/SBAD/4710.

Appendix A. Supplementary data

Supplementary data to this article can be found online at https://doi.org/10.1016/j.polymertesting.2021.107449.

References

[1] R.J. Crawford, J. Throne, Rotational Molding Technology, William Andrew Publishing, New York, 2001.
[2] K.O. Ogila, M. Shao, W. Yang, J. Tan, Rotational molding: a review of the models and materials, Express Polym. Lett. 11 (2017) 778–798, https://doi.org/10.3144/expresspolymlett.2017.75.
[3] S. Waigaonkar, B.J.C. Babu, R.T. Durai Prabhakaran, A new approach for resin selection in rotational molding, J. Reinforc. Plast. Compos. 27 (2008) 1021–1037, https://doi.org/10.1177/0731684407086629.
[4] S. Sarrabi, X. Colin, A. Tcharkhtchi, Kinetic modeling of polypropylene thermal oxidation during its processing by rotational molding, J. Appl. Polym. Sci. (2010), https://doi.org/10.1002/app.32459 n/a-n/a.
[5] A. Greco, A. Maffezzoli, S. Forleo, Rotational Molding of Bio-Polymers, 2014, pp. 333–337, https://doi.org/10.1063/1.4873794.
[6] A. Greco, F. Ferrari, A. Maffezzoli, Processing of super tough plasticized PLA by rotational molding, Adv. Polym. Technol. 2019 (2019) 1–8, https://doi.org/10.1155/2019/3835829.
[7] A. Greco, A. Maffezzoli, Rotational molding of poly(lactic acid): effect of polymer grade and granulometry, Adv. Polym. Technol. 36 (2017) 477–482, https://doi.org/10.1002/adv.21630.
[8] A. Vignali, S. Iannace, G. Falcone, R. Utzeri, P. Stagnaro, F. Bertini, Lightweight poly(ε-caprolactone) composites with surface modified hollow glass microspheres for use in rotational molding: thermal, rheological and mechanical properties, Polymers 11 (2019) 624, https://doi.org/10.3390/polym11040624.
[9] D. Garlotta, A literature review of poly(lactic acid), J. Polym. Environ. 9 (2001) 63–84, https://doi.org/10.1023/A:1020200822435.
[10] A. Masek, S. Cichosz, M. Piotrowska, Biocomposites of epoxidized natural rubber/poly(lactic acid) modified with natural fillers (Part I), Int. J. Mol. Sci. 22 (2021) 3150, https://doi.org/10.3390/ijms22063150.
[11] K. Mazur, S. Kuciel, K. Salasinska, Mechanical, fire, and smoke behaviour of hybrid composites based on polyamide 6 with basalt/carbon fibres, J. Compos. Mater. 53 (2019) 3979–3991, https://doi.org/10.1177/0021998319853015.
[12] V. Srebrenkoska, G. Bogoeva Gaceva, D. Dimeski, Biocomposites based on polylactic acid and their thermal behavior after recycing, Maced. J. Chem. Chem. Eng. 33 (2014) 277, https://doi.org/10.20450/mjcce.2014.479.
[13] W. Yan, R.J.T. Lin, D. Bhattacharyya, Particulate reinforced rotationally moulded polyethylene composites – mixing methods and mechanical properties, Compos. Sci. Technol. 66 (2006) 2080–2088, https://doi.org/10.1016/j.compscitech.2005.12.022.
[14] G. Höfler, R.J.T. Lin, K. Jayaraman, Rotational moulding and mechanical characterisation of halloysite reinforced polyethylenes, J. Polym. Res. 25 (2018) 132, https://doi.org/10.1007/s10965-018-1525-3.
[15] E.O. Cisneros-López, A.A. Pérez-Fonseca, Y. González-García, D.E. Ramírez-Arreola, R. González-Núñez, D. Rodrigue, J.R. Robledo-Ortíz, Polylactic acid-agave fiber biocomposites produced by rotational molding: a comparative study with compression molding, Adv. Polym. Technol. 37 (2018) 2528–2540, https://doi.org/10.1002/adv.21928.
[16] M.E. González-López, A.A. Pérez-Fonseca, E.O. Cisneros-López, R. Manríquez-González, D.E. Ramírez-Arreola, D. Rodrigue, J.R. Robledo-Ortíz, Effect of maleated PLA on the properties of rotomolded PLA-agave fiber biocomposites, J. Polym. Environ. 27 (2019) 61–73, https://doi.org/10.1007/s10924-018-1308-2.
[17] F.G. Torres, C.L. Aragon, Final product testing of rotational moulded natural fibre-reinforced polyethylene, Polym. Test. 25 (2006) 568–577, https://doi.org/10.1016/j.polymertesting.2006.03.010.
[18] B. Wang, S. Panigrahi, L. Tabil, W. Crerar, Pre-treatment of flax fibers for use in rotationally molded biocomposites, J. Reinforc. Plast. Compos. 26 (2007) 447–463, https://doi.org/10.1177/0731684406072526.
[19] M. Barczewski, M. Szostak, D. Nowak, A. Piasecki, Effect of wood flour addition and modification of its surface on the properties of rotationally molded polypropylene composites, Polimery 63 (2018) 772–784, https://doi.org/10.14314/polimery.2018.11.5.
[20] J. Andrzejewski, A. Krawczak, K. Wesoły, M. Szostak, Rotational molding of biocomposites with addition of buckwheat husk filler. Structure-property correlation assessment for materials based on polyethylene (PE) and poly(lactic acid) PLA, Compos. B Eng. 202 (2020), 108410, https://doi.org/10.1016/j.compositesb.2020.108410.
[21] A. Greco, A. Maffezzoli, Rotational molding of biodegradable composites obtained with PLA reinforced by the wooden backbone of opuntia ficus indica cladodes, J. Appl. Polym. Sci. 132 (2015), https://doi.org/10.1002/app.42447 n/a-n/a.
[22] L.D.V.E. León, V.A. Escocio, L.L.Y. Visconte, J.C.J. Junior, E.B.A.V. Pacheco, Rotomolding and polyethylene composites with rotomolded lignocellulosic materials: a review, J. Reinforc. Plast. Compos. 39 (2020) 459–472, https://doi.org/10.1177/0731684420916529.
[23] A.K. Bledzki, A.A. Mamun, J. Volk, Physical, chemical and surface properties of wheat husk, rye husk and soft wood and their polypropylene composites, Compos. Part A Appl. Sci. Manuf. 41 (2010) 480–488, https://doi.org/10.1016/j.compositesa.2009.12.004.
[24] S. Díaz, Z. Ortega, M. McCourt, M.P. Kearns, A.N. Benítez, Recycling of polymeric fraction of cable waste by rotational moulding, Waste Manag. 76 (2018) 199–206, https://doi.org/10.1016/j.wasman.2018.03.020.
[25] V. Girish Chandran, S.D. Waigaonkar, Mechanical properties and creep behavior of rotationally moldable linear low density polyethylene-fumed silica nanocomposites, Polym. Compos. 38 (2017) 421–430, https://doi.org/10.1002/pc.23600.
[26] V.G. Chandran, S.D. Waigaonkar, Rotational molding of linear low density polyethylene (LLDPE) fumed silica nanocomposites, Int. Polym. Process. 32 (2017) 50–57, https://doi.org/10.3139/217.3264.
[27] P. Bútora, A. Náplava, M. Ridzoň, J. Bílik, V. Tittel, Particle filled polyethylene composites used in the technology of rotational moulding, Res. Pap. Fac. Mater. Sci. Technol. Slovak Univ. Technol. 19 (2011) 9–18, https://doi.org/10.2478/v10186-011-0051-5.
[28] M. Daryadel, T. Azdast, M. Khatami, M. Moradian, Investigation of tensile properties of polymeric nanocomposite samples in the rotational molding process, Polym. Bull. (2020), https://doi.org/10.1007/s00289-020-03225-0.
[29] A.G. Spence, R.J. Crawford, The effect of processing variables on the formation and removal of bubbles in rotationally molded products, Polym. Eng. Sci. 36 (1996) 993–1009, https://doi.org/10.1002/pen.10487.
[30] T. Ouprara, K. Sangpradit, The development of rotational molding of waste bamboo powder with LLDPE plastic powder, E3S Web Conf. 187 (2020), 05003, https://doi.org/10.1051/e3sconf/202018705003.
[31] K. Murari, R. Siddique, K.K. Jain, Use of waste copper slag, a sustainable material, J. Mater. Cycles Waste Manag. 17 (2015) 13–26, https://doi.org/10.1007/s10163-014-0254-x.
[32] B. Gorai, R.K. Jana, Premchand, Characteristics and utilisation of copper slag—a review, Resour. Conserv. Recycl. 39 (2003) 299–313, https://doi.org/10.1016/S0921-3449(02)00171-4.
[33] K. Kambham, S. Sangameswaran, S.R. Datar, B. Kura, Copper slag: optimization of productivity and consumption for cleaner production in dry abrasive blasting, J. Clean. Prod. 15 (2007) 465–473, https://doi.org/10.1016/j.jclepro.2005.11.024.
[34] R. Sharma, R.A. Khan, Sulfate resistance of self compacting concrete incorporating copper slag as fine aggregates with mineral admixtures, Construct. Build. Mater. 287 (2021), 122985, https://doi.org/10.1016/j.conbuildmat.2021.122985.
[35] N. Suresh, M. M, Post-thermal properties of Portland cement concrete made with copper slag as fine aggregates, J. Struct. Fire Eng. ahead-of-p (2021), https://doi.org/10.1108/JSFE-06-2020-0018.
[36] S. Biswas, A. Satapathy, Use of copper slag in glass-epoxy composites for improved wear resistance, Waste Manag. Res. J. Sustain. Circ. Econ. 28 (2010) 615–625, https://doi.org/10.1177/0734242X09352260.
[37] G. Kalusuraman, S. Thirumalai Kumaran, M. Aslan, K. Mayandi, Mechanical properties of waste copper slag filled surface activated jute fiber reinforced composite, Mater. Res. Express 6 (2020), 125347, https://doi.org/10.1088/2053-1591/ab6089.
[38] A. Hejna, K. Piszcz-Karaś, N. Filipowicz, H. Cieśliński, J. Namieśnik, M. Marć, M. Klein, K. Formela, Structure and performance properties of environmentally-friendly biocomposites based on poly(ε-caprolactone) modified with copper slag and shale drill cuttings wastes, Sci. Total Environ. (2018) 640–641, https://doi.org/10.1016/j.scitotenv.2018.05.385, 1320–1331.
[39] Waste Management for the Food Industries, Elsevier, 2008, https://doi.org/10.1016/B978-0-12-373654-3.X5001-9.
[40] G. Gorrasi, R. Pantani, Hydrolysis and Biodegradation of Poly(lactic Acid), 2017, pp. 119–151, https://doi.org/10.1007/12_2016_12.
[41] S. Teixeira, K.M. Eblagon, F. Miranda, M.F.R. Pereira, J.L. Figueiredo, Towards controlled degradation of poly(lactic) acid in technical applications, C 7 (2021) 42, https://doi.org/10.3390/c7020042.
[42] A. Hejna, M. Barczewski, J. Andrzejewski, P. Kosmela, A. Piasecki, M. Szostak, T. Kuang, Rotational molding of linear low-density polyethylene composites filled with wheat bran, Polymers 12 (2020) 1004, https://doi.org/10.3390/polym12051004.
[43] Z. Ortega, M.D. Monzón, A.N. Benítez, M. Kearns, M. McCourt, P.R. Hornsby, Banana and Abaca fiber-reinforced plastic composites obtained by rotational molding process, Mater. Manuf. Process. (2013), 130614085148001, https://doi.org/10.1080/10426914.2013.792431.
[44] R.C. Vázquez Fletes, E.O. Cisneros López, F.J. Moscoso Sánchez, E. Mendizábal, R. González Núñez, D. Rodrigue, P. Ortega Gudiño, Morphological and mechanical properties of bilayers wood-plastic composites and foams obtained by rotational molding, Polymers 12 (2020) 503, https://doi.org/10.3390/polym12030503.
[45] R. Shaker, D. Rodrigue, Rotomolding of thermoplastic elastomers based on low-density polyethylene and recycled natural rubber, Appl. Sci. 9 (2019) 5430, https://doi.org/10.3390/app9245430.
[46] M. Barczewski, P. Wojciechowska, M. Szostak, Mechanical Properties and Structure of Reactive Rotationally Molded Polyurethane - Basalt Powder Composites, 2019, https://doi.org/10.1007/978-3-030-16943-5_52.

[47] E.W. Fischer, H.J. Sterzel, G. Wegner, Investigation of the structure of solution grown crystals of lactide copolymers by means of chemical reactions, Kolloid-Z. Z. Polym. 251 (1973) 980–990, https://doi.org/10.1007/BF01498927.
[48] J. Liu, R. Guo, Hydration properties of alkali-activated quick cooled copper slag and slow cooled copper slag, J. Therm. Anal. Calorim. 139 (2020) 3383–3394, https://doi.org/10.1007/s10973-019-08708-5.
[49] A. Nazer, J. Payá, M.V. Borrachero, J. Monzó, Use of ancient copper slags in Portland cement and alkali activated cement matrices, J. Environ. Manag. 167 (2016) 115–123, https://doi.org/10.1016/j.jenvman.2015.11.024.
[50] J.P. Mofokeng, A.S. Luyt, T. Tábi, J. Kovács, Comparison of injection moulded, natural fibre-reinforced composites with PP and PLA as matrices, J. Thermoplast. Compos. Mater. 25 (2012) 927–948, https://doi.org/10.1177/0892705711423291.
[51] R. Auras, B. Harte, S. Selke, An overview of polylactides as packaging materials, Macromol. Biosci. 4 (2004) 835–864, https://doi.org/10.1002/mabi.200400043.
[52] V. Katiyar Monika, Non-isothermal degradation kinetics of PLA-functionalized gum (fG) biocomposite with dicumyl peroxide (DCP), J. Therm. Anal. Calorim. 138 (2019) 195–210, https://doi.org/10.1007/s10973-019-08231-7.
[53] E.E. Popa, M. Rapa, O. Popa, G. Mustatea, V.I. Popa, A.C. Mitelut, M.E. Popa, Polylactic acid/cellulose fibres based composites for food packaging applications, Mater. Plast. 54 (2017) 673–677, https://doi.org/10.37358/MP.17.4.4923.
[54] B.E. Arteaga-Ballesteros, A. Guevara-Morales, E.S. Martín-Martínez, U. Figueroa-López, H. Vieyra, Composite of polylactic acid and microcellulose from kombucha membranes, E-Polymers 21 (2020) 15–26, https://doi.org/10.1515/epoly-2021-0001.
[55] A.A. Cuadri, Thermal , thermo-oxidative and thermomechanical degradation of PLA : a comparative study based on rheological , chemical and thermal properties, Polym. Degrad. Stabil. 150 (2018) 37–45, https://doi.org/10.1016/j.polymdegradstab.2018.02.011.
[56] X. Liu, Y. Zou, W. Li, G. Cao, W. Chen, Kinetics of thermo-oxidative and thermal degradation of poly(d,l-lactide) (PDLLA) at processing temperature, Polym. Degrad. Stabil. 91 (2006) 3259–3265, https://doi.org/10.1016/j.polymdegradstab.2006.07.004.
[57] M. Barczewski, O. Mysiukiewicz, D. Matykiewicz, K. Skórczewska, K. Lewandowski, J. Andrzejewski, A. Piasecki, Development of polylactide composites with improved thermomechanical properties by simultaneous use of basalt powder and a nucleating agent, Polym. Compos. 41 (2020) 2947–2957, https://doi.org/10.1002/pc.25589.
[58] M.J. Fernández, M.D. Fernández, I. Aranburu, Poly(l-lactic acid)/organically modified vermiculite nanocomposites prepared by melt compounding: effect of clay modification on microstructure and thermal properties, Eur. Polym. J. 49 (2013) 1257–1267, https://doi.org/10.1016/j.eurpolymj.2013.02.031.
[59] V. Kumar, A. Dev, A.P. Gupta, Studies of poly(lactic acid) based calcium carbonate nanocomposites, Compos. B Eng. 56 (2014) 184–188, https://doi.org/10.1016/j.compositesb.2013.08.021.
[60] J.-M. Raquez, Y. Habibi, M. Murariu, P. Dubois, Polylactide (PLA)-based nanocomposites, Prog. Polym. Sci. 38 (2013) 1504–1542, https://doi.org/10.1016/j.progpolymsci.2013.05.014.
[61] M. Ghozali, E. Triwulandari, Y. Meliana, S. Fahmiati, W. Fatriasari, R.P.B. Laksana, N. Masruchin, L. Suryanegara, Thermal Properties of Polylactic Acid/zinc Oxide Biocomposite Films, 2018, 020032, https://doi.org/10.1063/1.5064318.
[62] M. Murariu, A. Doumbia, L. Bonnaud, A. Dechief, Y. Paint, M. Ferreira, C. Campagne, E. Devaux, P. Dubois, High-performance polylactide/ZnO nanocomposites designed for films and fibers with special end-use properties, Biomacromolecules 12 (2011) 1762–1771, https://doi.org/10.1021/bm2001445.
[63] M.J. Oliveira, M.C. Cramez, Rotational molding OF polyolefins: processing, morphology, and properties, J. Macromol. Sci. Part B. 40 (2001) 457–471, https://doi.org/10.1081/MB-100106170.
[64] M. Barczewski, O. Mysiukiewicz, Rheological and processing properties of poly (lactic acid) composites filled with ground chestnut shell, Polym. Korea 42 (2018) 267–274, https://doi.org/10.7317/pk.2018.42.2.267.
[65] J. Li, C. Zhou, G. Wang, D. Zhao, Study on rheological behavior of polypropylene/clay nanocomposites, J. Appl. Polym. Sci. 89 (2003) 3609–3617, https://doi.org/10.1002/app.12643.
[66] B.I. Chaudhary, E. Takács, J. Vlachopoulos, Processing enhancers for rotational molding of polyethylene, Polym. Eng. Sci. 41 (2001) 1731–1742, https://doi.org/10.1002/pen.10870.
[67] N. Le Moigne, M. van den Oever, T. Budtova, Dynamic and capillary shear rheology of natural fiber-reinforced composites, Polym. Eng. Sci. 53 (2013) 2582–2593, https://doi.org/10.1002/pen.23521.
[68] M. Koleva, V. Vassilev, G. Vassilev, Polymer composites containing waste dust from power production II. Strength characteristics of composites based on UPR/HIPS polymer system, Maced. J. Chem. Chem. Eng. 27 (2008) 47, https://doi.org/10.20450/mjcce.2008.246.
[69] M. Masłowski, J. Miedzianowska, K. Strzelec, Natural rubber composites filled with crop residues as an alternative to vulcanizates with common fillers, Polymers 11 (2019) 972, https://doi.org/10.3390/polym11060972.
[70] A. Hejna, Poly(ε-Caprolactone)/Brewers' spent grain composites—the impact of filler treatment on the mechanical performance, J. Compos. Sci. 4 (2020) 167, https://doi.org/10.3390/jcs4040167.
[71] A. Hejna, M. Barczewski, P. Kosmela, O. Mysiukiewicz, A. Kuzmin, Coffee silverskin as a multifunctional waste filler for high-density polyethylene green composites, J. Compos. Sci. 5 (2021) 44, https://doi.org/10.3390/jcs5020044.
[72] M.I. Baumer, J.L. Leite, D. Becker, Influence of calcium carbonate and slip agent addition on linear medium density polyethylene processed by rotational molding, Mater. Res. 17 (2013) 130–137, https://doi.org/10.1590/S1516-14392013005000159.
[73] M.C. Kuo, C.M. Tsai, J.C. Huang, M. Chen, PEEK composites reinforced by nano-sized SiO2 and Al2O3 particulates, Mater. Chem. Phys. 90 (2005) 185–195, https://doi.org/10.1016/j.matchemphys.2004.10.009.
[74] J. Exner, M. Schubert, D. Hanft, T. Stöcker, P. Fuierer, R. Moos, Tuning of the electrical conductivity of Sr(Ti,Fe)O3 oxygen sensing films by aerosol co-deposition with Al2O3, Sensor. Actuator. B Chem. 230 (2016) 427–433, https://doi.org/10.1016/j.snb.2016.02.033.
[75] M. Heşami, A. Jalali-Arani, Cold crystallization behavior of poly(lactic acid) in its blend with acrylic rubber; the effect of acrylic rubber content, Polym. Int. 66 (2017) 1564–1571, https://doi.org/10.1002/pi.5414.
[76] B.J.A. Gutierrez, S. Dul, A. Pegoretti, J. Alvarez-Quintana, L. Fambri, Investigation of the effects of multi-wall and single-wall carbon nanotubes concentration on the properties of ABS nanocomposites, C 7, 2021, p. 33, https://doi.org/10.3390/c7020033.
[77] J.F. Balart, D. García-Sanoguera, R. Balart, T. Boronat, L. Sánchez-Nacher, Manufacturing and properties of biobased thermoplastic composites from poly (lactid acid) and hazelnut shell wastes, Polym. Compos. 39 (2018) 848–857, https://doi.org/10.1002/pc.24007.